INTERNATIONAL ATOMIC ENERGY AGENCY
UNITED NATIONS EDUCATIONAL, SCIENTIFIC AND CULTURAL ORGANIZATION
INTERNATIONAL CENTRE FOR THEORETICAL PHYSICS
I.C.T.P., P.O. BOX 586, 34100 TRIESTE, ITALY, CABLE: CENTRATOM TRIESTE

SMR.764 - 3

RESEARCH WORKSHOP ON CONDENSED MATTER PHYSICS
13 JUNE - 19 AUGUST 1994

WORKING GROUP ON "DISORDERED ALLOYS"
8 - 19 AUGUST 1994

"An augmented space recursive technique for the analysis of alloy phase stability in random binary alloys

Part II

Abhijit MOOKERJEE
S.N. Bose National Centre for Basic Sciences
DB17, Sector 1, Salt Lake City
Calcutta 700064
INDIA

LECTURE 2

AN AUGMENTED SPACE RECURSIVE TECHNIQUE FOR THE ANALYSIS OF ALLOY PHASE STABILITY IN RANDOM BINARY ALLOYS

ABHIJIT MOOKERJEE
S. N. Bose National Centre for Basic Sciences.
DB 17, Sector 1, Salt Lake City, Calcutta 700064, INDIA

9 August, 1994

Abstract

In this lecture we shall introduce the augmented-space recursion method coupled with the orbital peeling technique, as a powerful tool for the calclulation of effective cluster interactions, useful for the study of alloy phase stability. An application to the well studied PdV system has been carried out.

1 INTRODUCTION.

In recent years, there has been considerable interest in the first principle calculation of alloy ordering tendencies at T = 0°K. In order to understand the onset of ordering in random alloys , one needs a derivation of the lowest configurational energy for a specified alloy system. Models have been formulated to represent the configurational energies in terms of effective multisite interactions , in particular effective pair interactions [1]. Within this approach, the analysis of alloy ordering tendencies and phase stability reduces to the accurate and reliable determination of effective pair interactions . Traditionally there has been two different approaches of obtaining the effective pair interactions. The first approach is to start with the electronic structure calculation and total energy determination of ordered super-structures of the alloy and to invert these total energies to get the effective pair potentials by the Connolly-Williams method [2] . The other approach is to start with the disordered phase , set up a perturbation in the form of concentration fluctuations associated with an ordered phase and study whether the alloy can sustain such a perturbation. This approach includes the generalized perturbation method (GPM)[3], the embedded cluster method (ECM)[4] and the concentration wave approach [5]. Most of the work on the electronic structure of the disordered alloys has been based so far on the coherent potential approximation (CPA). The CPA being a single-site approximation has its own limitations. In addition , self-consistency involved in it invokes subtle convergence procedures at each energy point.

Analytic generalizations beyond the single site CPA, like the Cluster CPA [6] based on the augmented space formalism and the Travelling Cluster Approximation [7] are beset with computational difficulties when cluster sizes are large. Los *et. al.* [8] have proposed a cluster expansion of the multiple scattering t-matrix. However, the analyticity preserving property of the truncated expansion has not been established as yet. In a separate attempt to go beyond the single site approximation , de Fontaine and his group followed a different approach of direct configurational averaging (DCA) [9], without resorting to any kind of single-site approximation. The effective pair and multisite interactions were calculated directly in real space for given configurations and the averaging was done , brute force, as it were, by summing over different configurations.

The augmented space formalism (ASF) put forward by one of us [10] provides a convenient means of configuration averaging which is not restricted by the above limitations. In a recent communication [11] we have shown that the ASF coupled with the recursion technique of Haydock *et. al.* [12] successfully reproduces the electronic density of states of random alloys without resorting to single site approximations and does not require the self-consistency loops of CPA and its generalizations. The aim of the present work is to employ this methodology to get effective pair interactions. Within the ASF, configuration averaging is done exactly, while the approximation within the subsequent recursion on augmented space can be carried out in a controlled manner and the estimates of errors produced have been carefully studied [13]. One works directly in real space, augmented with the space of configurations and does away with the limitations of the k-space super cell methods. Since the pair interactions are differences in total energies of different pairs in the alloy medium, they can be obtained directly by the orbital peeling method, without going through large subtractive cancellation [14].

The main points of our methodology are (i) the application of the tight-binding linearized muffin-tin-orbital method (TB-LMTO) [15] in conjunction with augmented space recursion to describe the electronic structure of random alloys ; (ii) the application of the orbital peeling technique for the determination of the pair-potential; (iii) the use of the ground state analysis of the 3D Ising model of Kanamori and Kakehashi [16] to discuss the stability properties of alloys. In the present communication we have explained the usefulness of this method and have employed the method to study the phase stability of Pd-V system at three different alloy compositions.

2 FORMALISM.

2.1 EFFECTIVE PAIR INTERACTIONS.

The starting point of our calculation is the expansion of the configuration energy in terms of effective cluster interactions. The expansion for the configuration energy E for a binary alloy A_cB_{1-c} may be written as :

$$E(P_i) \;=\; E^{(0)} \;+\; \sum_{i=1}^{N} E_i^{(1)}\delta c_i \;+\; \sum_{i,j=1}^{N} E_{ij}^{(2)}\delta c_i \delta c_j \;+\; \cdots \tag{1}$$

If n_i are the occupation probabilities for the A type of atom, δc_i is the concentration fluctuation given by $n_i - c$, where $c = \langle P_i \rangle$. The coefficients $E^{(0)}$, $E^{(1)}$ ... are the effective renormalized cluster interactions (renormalized in the sense that contributions from self-retraced paths have been included). $E^{(0)}$ is the energy of the averaged disordered medium, $E_i^{(1)}$ is the interchange energy for the species A and B, and it defines the single body interaction resulting from the interchange of a B atom with an A atom at site i in the alloy, $E_{ij}^{(2)}$ is the effective renormalized pair interaction which is the difference in the single body interaction at i, when sites j ($\neq$ i) is occupied either by A or B atom.

The renormalized pair interactions express the correlation between two sites and are the most dominant quantities for the analysis of phase stability. We will retain terms up to pair interactions in the configuration energy expansion. Higher order interactions may be included for a more accurate and complete description.

At this point it is worth mentioning that our scheme of calculation of the renormalized pair interactions is similar to other methods based on embedding clusters in an effective medium. The calculation involves the determination of the electronic structure as well as averaging over different configurations of the system. It is precisely in this averaging scheme that the different methods based on the embedding method differ from one another. In the CPA-ECM the averaging is done within the framework of the CPA. In the DCA the averging is done directly by summing over different random configurations. If the configurations are consistent with a particular concentration *alone* the method is called the *canonical* DCA [17]. If averaging is done over all configurations as well as all possible concentrations, the method is called the *grand canonical* DCA [18]. In our scheme we employ the augmented space recursion for carrying out configuration averaging.

The other commonly used approach for obtaining the effective cluster interactions is the GPM. The equivalence of the CPA-ECM and the properly renormalized GPM (which is a CPA based technique) has been established previously and , in fact, the CPA-ECM gives the exact summation of the partially renormalized GPM to all orders [1]. A detailed comparison of the various methods will be made later in the section on Discussions.

The total energy of a solid may be separated into two terms : a one-electron band contribution E_{BS} and an electrostatic term E_{ES} which includes several contributions : the Coulomb repulsion of the ion cores, the correction for double counting terms due to electron-electron interaction in E_{BS} and a Madelung energy in case the solid has ionic character. The renormalized cluster interactions defined in (1) should, in principle, include both E_{BS} and E_{ES} contributions. Since the renormalized cluster interactions involve the difference of cluster energies, it is usually assumed that the electrostatic terms cancel out and only the band structure contribution is important. Obviously, such an assumption is not rigorously true, but it has been shown to be approximately valid in a number of alloy systems (including PdV which we study here) [19]. Most of the works where calculations start from the disordered side are based on the band structure contribution alone. Our work also has that assumption.

The effective pair interactions can be related to the change in the configuration averaged local density of states :

$$E_{ij}^{(2)} \;=\; \int_{-\infty}^{E_F} dE(E-E_F)\Delta n(E) \tag{2}$$

where Δn(E) is given by :

$$\Delta n(E) \;=\; \sum_{IJ\in \text{all pairs}} Im\langle Tr(E\mathbf{I}-\mathbf{H}^{IJ})^{-1}\rangle \xi_{IJ} \tag{3}$$

ξ_{IJ} is $\pm$ 1 according to whether I=J or I$\neq$ J and $\langle\ldots\rangle$ refer to configuration averaging.

There are four possible pairs which IJ can be : AA, AB, BA and BB. H^{IJ} is the Hamiltonian of a system where all sites except i and j are randomly occupied, whereas the sites i and j are occupied by atoms of the type I and J. This change in the averaged local density of states can be related to the generalized phase shift η(E) through the equation :

$$\Delta n(E) \;=\; \frac{d\eta(E)}{dE} \tag{4}$$

where $\eta(E)$ is :

$$\eta(E) \;=\; \log \frac{\det < G^{AA} > \det < G^{BB} >}{\det < G^{AB} > \det < G^{BA} >} \tag{5}$$

G^{IJ} is the resolvent of the hamiltonian H^{IJ}. The generalized phase shift $\eta(E)$ can easily be calculated following the orbital peeling method of Burke [14]. The details of the orbital peeling method in the context of pair interaction has been mentioned in detail elsewhere [9], and here we shall quote only the final result :

$$\begin{aligned} E_{ij}^{(2)} &= \sum_{IJ\epsilon \text{all pairs}} \sum_{\alpha=1}^{9} \xi_{IJ} \int_{-\infty}^{E_F} (E-E_F) \log < G_\alpha^{IJ} > \\ &= \sum_{IJ\epsilon \text{all pairs}} \sum_{\alpha=1}^{9} \left[\sum_{k=1}^{p-1} Z_k^{\alpha,IJ} - \sum_{k=1}^{p} P_k^{\alpha,IJ} + \left(N_P^{\alpha,IJ} - N_Z^{\alpha,IJ} \right) E_F \right] \end{aligned} \tag{6}$$

where G$_\alpha^{IJ}$ denotes the Green function corresponding to the Hamiltonian , where two atoms are embedded at sites I and J in which the orbitals from 1 to (α - 1) are deleted at the site I. Z$_k^{\alpha,IJ}$ and P$_k^{\alpha,IJ}$ are the zeros and poles of G$_\alpha^{IJ}$. N$_Z^{\alpha,IJ}$ and N$_P^{\alpha,IJ}$ are the number of such zeros and poles below E$_F$. This method of zeros and poles enables one to carry out the integration easily avoiding the multivaluedness of the integrand involved in the evaluation of the integral by parts. These zeros and poles are estimated from the recursion coefficients for ¡G$_\alpha^{IJ}$ >.

2.2 AUGMENTED SPACE RECURSION

As discussed in the previous section, the calculation of the effective pair interaction in our formalism reduces to the determination of the configuration averaged green functions $\langle G^{AA}\rangle$, $\langle G^{BB}\rangle$,$\langle G^{AB}\rangle$ and $\langle G^{BA}\rangle$. We shall employ the augmented space recursion coupled with the linearized tight-binding muffin tin orbital method (TB-LMTO) introduced by Anderson and Jepson [15] for a first principle determination of these configuration averaged quantitles. We shall take the most localized, sparse tight binding Hamiltonian derived systematically from the LMTO-ASA theory and generalized to random alloys, given by :

$$\begin{aligned} H^{\beta}_{iL,jL'} &= C'_{iL}\delta_{iL}\delta_{jL'} + \Delta^{1/2}_{iL}S^{\beta}_{iLjL'}\Delta^{1/2}_{jL'} \\ C'_{iL} &= C^{A}_{L}n_i + C^{B}_{L}(1-n_i) \\ \Delta^{1/2}_{L} &= \left(\Delta^{1/2}_{L}\right)^{A} n_i + \left(\Delta^{1/2}_{L}\right)^{B}(1-n_i) \end{aligned} \tag{7}$$

Here i,j denote the lattice sites and L=(ℓm) are the orbital indices (for transition metal $\ell \leq 2$). C^A_L,C^B_L Δ^A_L and Δ^B_L are the potential parameters of the constituents A and B of the alloy, n_i are the local site-occupation variables which randomly take values 0 or 1 according to whether the site is occupied by an A atom or not. The screened or tight binding structure function S^β contains all the information on lattice geometry, and it is expressed in terms of conventional structure function S^0 and the screening parameter β as

$$S^{\beta} = S^{0}(1+\beta S^{\beta}) \tag{8}$$

The Hamiltonian described by equation (7) is related to the nearly orthonormal γ-representation by the relation

$$H^{\gamma} = E_{\nu} + h^{\gamma} = E_{\nu} + h^{\beta} - h^{\beta}o^{\beta}h^{\beta} + \ldots \tag{9}$$

This ASA form of the orthonormalised Hamiltonian was used in the present work. Usually the expansion is truncated after the second term which is accurate to first order in (E-E$_\nu$). The third term is necessary for systems with wide bands specially for s,p states. We have used both first and second order approximations to ensure convergence. The configuration averaged green functions $\langle G_\alpha^{IJ}(z)\rangle$ is $\langle (zI - H^{IJ})^{-1}\rangle$. Assuming that we embed I and J in sites 1 and 2 the Hamiltonian H$_\alpha^{IJ}$ has the following form:

$$\begin{aligned}
H_\alpha^{IJ} \;=\; & \sum_{\ell=\alpha}^{9} C_{1,\ell}^{I} a_1^\dagger a_1 + \sum_{\ell=1}^{9} C_{2,\ell}^{J} a_2^\dagger a_2 + \ldots \\
+ \; & \sum_{p\neq 1,2} \sum_{\ell=1}^{9} \left(C_{p,\ell}^{B} + \delta C_\ell n_p \right) a_p^\dagger a_p + \ldots \\
+ \; & \sum_{p\neq 1} \sum_{\ell=\alpha}^{9} \sum_{\ell'=1}^{9} \Delta_{1,\ell}^{1/2,I} S_{\ell,\ell'}^{1,p} \left(\Delta_{p,\ell'}^{1/2,B} + \delta\Delta_{\ell'}^{1/2} n_p \right) a_1^\dagger a_p \ldots \\
+ \; & \sum_{p\neq 2} \sum_{\ell=1}^{9} \sum_{\ell'=1}^{9} \Delta_{2,\ell}^{1/2,I} S_{\ell,\ell'}^{2,p} \left(\Delta_{p,\ell'}^{1/2,B} + \delta\Delta_{\ell'}^{1/2} n_p \right) a_2^\dagger a_p \ldots \\
+ \; & \sum_{p\neq 1} \sum_{\ell=1}^{9} \sum_{\ell'=\alpha}^{9} \left(\Delta_{p,\ell}^{1/2,B} + \delta\Delta_{\ell}^{1/2} n_p \right) S_{\ell,\ell'}^{p,1} \Delta_{1,\ell'}^{1/2,I} a_p^\dagger a_1 \ldots \\
+ \; & \sum_{p\neq 2} \sum_{\ell=1}^{9} \sum_{\ell'=1}^{9} \left(\Delta_{p,\ell}^{1/2,B} + \delta\Delta_{\ell}^{1/2} n_p \right) S_{\ell,\ell'}^{p,2} \Delta_{2,\ell'}^{1/2,I} a_p^\dagger a_2 \ldots \\
+ \; & \sum_{p\neq 1,2} \sum_{q\neq 1,2} \sum_{\ell=1}^{9} \sum_{\ell'=1}^{9} \left(\Delta_{p,\ell}^{1/2,B} + \delta\Delta_{\ell}^{1/2} n_p \right) S_{\ell,\ell'}^{p,q} \left(\Delta_{q,\ell'}^{1/2,B} + \delta\Delta_{\ell'}^{1/2} n_q \right) \\
& (a_p^\dagger a_q + a_q^\dagger a_p)
\end{aligned} \tag{10}$$

We note that the Hamiltonian has both diagonal as well as off diagonal disorder. We will retain this form of the Hamiltonian, and will not resort to any transformation as is done in single site approximations [20]. In order to evaluate the configuration average we will employ the ideas of the ASF which puts configuration averaging on the same footing as quantum mechanical averaging by augmenting the hilbert space spanned by the wave functions with a configuration space spanned by different realizations of the random variables associated with the Hamiltonian.

Let us suppose that the Hamiltonian describing the system is characterized by a set of random occupation variables $\{n_i\}$, which are independent. The probability density of the variables n_i is assumed to have finite moments of all orders, so that we may write

$$p(n_i) \;=\; \frac{1}{\pi}\langle\gamma_0^i|\left((n_i - i0)\mathbf{I} - \mathbf{M}^i\right)^{-1}|\gamma_0^i\rangle$$

where $\mathbf{M}^i$ is an operator defined on the configuration space ϕ^i of rank N , spanned by N possible realizations of n_i. The Augmented Space Theorem [10] now states that the configuration average of the resolvent G(E,$\{n_i\}$) may be written as

$$\langle G(E,\{n_i\})\rangle \;=\; \langle F|(z\tilde{I} - \tilde{H}(\{\tilde{M}^i\})^{-1}|F\rangle$$

$\tilde{\mathrm{H}}(\{\tilde{\mathrm{M}}^i\})$ is the same operator function in the augmented space of $\tilde{\mathrm{M}}^i$ as H($\{n_i\}$) was of n_i and $|F\rangle = \prod^{\otimes}|\gamma_0^i\rangle$ is the configuration ground state in the augmented space. Thus the configuration averaging has been reduced to the problem of the ground state matrix element in the augmented space $\Psi = H \otimes \Phi$. For a system with N sites and disorder described by binary probability distribution the rank of the space is N × 2^N.

The construction of $\tilde{\mathrm{M}}^i$ given the distribution of n_i has been described in detail earlier [10]. For a binary distribution $\tilde{\mathrm{M}}^i$ is given by:

$$\tilde{M}^i \;=\; x b_{i0}^{\dagger}b_{i0} + (1-x)b_{i1}^{\dagger}b_{i1} + \sqrt{x(1-x)}\left(b_{i0}^{\dagger}b_{i1} + b_{i1}^{\dagger}b_{i0}\right) \tag{10}$$

($\mathrm{b}_{i0}^{\dagger}$,$\mathrm{b}_{i0}$) and ($\mathrm{b}_{i1}^{\dagger}$,$\mathrm{b}_{i1}$) are the creation and annihilation operators in the augmented space where each site is characterized by two states (0,1) ,which may be identified with the up and down states of an Ising system. The configuration states may then be stored extremely efficiently in bits of words and the algebra of the Hamiltonian in the configuration space may mirror the multispin coding techniques used in numerical work with the Ising model.

Once we have identified the operators in the configuration space , it is worth while mentioning how one represents the basis in real and configuration spaces . A basis $|m\rangle$

in H is represented by a column vector C_m with zeros everywhere except at the m-th position. The inner product

$$\begin{aligned} \langle m| \odot |n\rangle &= C_m^T C_n \\ a_m^\dagger a_n C_p &= \delta_{np} C_m \end{aligned}$$

A member of the basis in $\prod_i^{\otimes} \phi_i$ has the form $|\gamma^1_{\lambda_1} \otimes \gamma^2_{\lambda_2} \cdots \otimes \gamma^j_{\lambda_j} \otimes \ldots\rangle$ where each λ may be either 0 or 1. In the usual terminology of ASF the number C of 1's defines the *cardinality* of the basis and the sequence of positions at which we have the 1's $\{S_C\}$ called the *cardinality sequence* labels the basis. Thus a binary sequence B[C,$\{S_C\}$] is a representation of the member of the basis in the configuration space. The dot product between these basis members is then

$$B[C, \{S_C\}] \odot B[C', \{S_{C'}\}] = \delta_{CC'} \delta\{S_C S_{C'}\}$$

Without going into the computational details we mention that the operations of $\tilde{\mathrm{H}}$ on the configuration space amount to changing cardinally and cardinality sequences . Since the operations are restricted to the bits of words one can easily employ logical functions to define the operation of the Hamiltonian in the configuration space.

It is well known, that for a system described by a sparse Hamiltonian the recursion method is one of the widely used methods to generate a continued fraction expansion of the resolvent of the Hamiltonian. Haydock[21] has mapped the contribution to the continued fraction coefficients to self-avoiding walks on the underlying space. He has shown that the dominant contribution comes from walks that wind round the initial starting state. This allows us to work only on a finite part of the augmented space. In practice the continued fraction is evaluated to a finite number of steps and then terminated by incorporating analyticity preserving terminators. Several terminators are available in the literature and we have chosen to use the terminator of Lucini and Nex [22]. The advantage of such a termination procedure is that the approximate resolvent retains the herglotz properties. It is interesting to compare this with the fact that in the cluster generalizations of the

CPA one goes to great lengths to ensure herglotzicity and these approximations cannot maintain the accuracy in the band widths. The terminator approximation preserves the first 2(N-2) moments of the density of states *exactly*. This represents the effect of a cluster at a distance (N-2) from the starting state. It also maintains the correct band-widths, band-weights and the correct singularities at the band edges. If we carry out recursion on the augmented space, we can compute the configuration averaged green function directly. The method does not involve single site approximations and solution of self-consistent equations as required in the CPA and its generalizations. For non-isochoric alloys , the difference in atomic radii of the constituents lead to change in the electronic density of states, as confirmed by experiment [23] and approximate theoretical techniques [24]. One thus expects that the mismatch of size produces, in addition to a relaxation energy E_R contribution, a change in the band structure. Within our Augmented Space Recursion (ASR), off-diagonal disorder in the structure matrix S^β because of local lattice distortions due to size mismatch of the constituents, can be handled on the same footing as diagonal disorder in the potential parameters [25].

The augmented space recursion with the TB-LMTO Hamiltonian coupled with orbital peeling allows us to compute configuration averaged pair-potentials directly, without resorting to any direct averaging over several configurations. In an earlier communication [11] we have discussed how one uses the local symmetries of the augmented space to reduce the Hamiltonian and carry out the recursion on a reducible subspace of much lower rank. If we fix the occupation of two sites, the local symmetry of the augmented space is lowered (this is very similar to the lowering of spherical symmetry to cylindrical symmetry when a preferred direction is introduced in an isotropic system). We may then carry out the recursion in a suitably reduced subspace.

3 RESULTS AND DISCUSSIONS.

We have applied the formalism developed in the previous section in calculating the pair potentials for the fcc based Pd_cV_{1-c} alloys for various values of the concentration c. The calculation of the pair potential has been restricted upto fourth neighbour interactions. Our choice of the Pd-V alloy is motivated by the fact, that in transition metal alloys (apart from few exceptions) the d band arguments show that the most strongly ordered alloys will have an average band filling near the middle of the d-band, or somewhere near five d-electrons, whereas alloys with band filling close to completely empty or full d level will tend towards phase separation. Pd-V alloys, with constituents on opposite ends of the transition metal series, will order according to the above prescription. Further, stability properties of Pd-V system is well studied both experimentally as well as by theoretical methods like KKR-CPA coupled with generalized perturbation method[26] and by LMTO coupled with direct configurational averaging[9], so reliable results are available for comparison with our predictions.

We now mention briefly some details concerning the numerical part of the problem . Total energy density-functional calculations were performed for Pd and V in the fcc-structure. The Kohn-Sham eqations were solved in the local-density approximations (LDA). The LDA was treated within the context of the method of the linear muffin-tin orbitals (LMTO) in the atomic sphere approximation. The computations were performed semi-relativistically (including scalar relativistic corrections) and the exchange-correlation potential of Von Barth and Hedin was used. The basis set was composed of ℓ = 0,1,2 orbitals , so that the occurring matrices were of order 9 . The potential parameters Δ_ℓ^I and γ_ℓ^I of the constituent I were scaled by the factors $(s^I/s^{alloy})^{2\ell+1}$ to account for the fact that the Wigner-Seitz radius of constituent I, s^I is different from that of the alloy, s^{alloy}. These potential parameters were used to parameterize the alloy Hamiltonian. This choice of different Wigner-Seitz radius for Pd and V allowed one to take into account charge self-consistency approximately, yet accurately and consistently, as emphasized by Kudrunovský *et. al.* [20]. For the purpose of augmented space recursion , a four shell augmented space map was generated from a cluster of 400 sites. We calculated the local density of states and fermi-energy with second order LMTO-ASA Hamiltonian through the recursion method exact upto eight levels of recursion. and with analytic terminator of Lucini and Nex[22] .

Figure 1 shows the total density of states for Pd-V alloy, for various concentrations with the positions of the fermi level shown. In order to maintain accuracy the Fermi energy E_F has been calculated from the second order Hamiltonian. For the calculation of the pair potential we followed the same methodology coupled with orbital peeling discussed in detail earlier with first order Hamiltonian. We found that since pair potentials are differences of integrated quantities, there seemd to be little appreciable change in doing the calculation with the second order Hamiltonian.

In Figure 2 we have plotted the nearest neighbour effective pair interactions, as functions of (a) band filling and (b) energy, at three different concentrations for the Pd-V alloy. The relation between the two figures can be understood by looking at the variation of the number of states per spin with energy. This is shown in Fig 2(c). The shape of the curves is in agreement with those obtained by other methodologies [9, 1], consisting of a phase separating region at the band edges and an ordering region near the centre. The magnitude of the effective pair interaction decreases with distance with increasing number of nodes.

In Figure 3 we have plotted V_1,V_2,V_3 and V_4 [1] for c = 0. 5 as a function of band filling to demonstrate this point. This in turn indicates the rapidly convergent properties of the configuration energy expanded in terms of effective cluster interactions. We find that $| V_1| \gg |V_2, V_3$ or $V_4|$. so that the ordered structures appear only when $V_1 > 0$.

Once we have obtained the effective pair interactions , they can be used to calculate the ordering energy , hence the relative stability of various ordered phases at a given concentration. At this point one can calculate the ordering energy expressed in terms of effective pair interactions for various stable phases at a given concentration to analyze the stability properties . However to discuss the stability properties of Pd-V alloy we will follow the method of Kanamori and Kakehashi [16] and calculate the antiphase boundary energy. Using the method of geometric inequalities these authors determined the ground

---

[1] $V_n = E^2_{ij}$, $|r_i - r_j| = na$ where a is the lattice constant

k	1	2	3	4	c
LI_2	0	3	0	6	0. 25
DO_{22}	0	2	4	2	0. 25
LI_0	2	3	4	6	0. 5
A_2B_2	2	2	8	2	0. 5

Table 1: Values of p_k for various superstructures at concentrations 0. 25 and 0. 5

state of 3D Ising model including pair interaction up to fourth NN interactions . They expressed the configurational energy as : $E_C = \sum_k V_k\, p_k$, where p_k is the total number of k-th neighbouring BB pairs in a given configuration C. The antiphase boundary energy between two closely related ordered superstructure configurations C and C′ is given by $\epsilon = E_C - E_{C'}$. In Table 1 we list the values of p_k/Nc for different configurations.

In Figure 4 we have plotted this anti-phase boundary energy $\epsilon = - V_2 + 4V_3 - 4V_4$ as a function of band filling for Pd-V with c = 0. 25, 0.5 and 0.75. The number of zeros is in agreement with the arguments based on moments (there has to be at least four zeros) . In the fcc lattice for c = 0. 75, the only possible ground states in the presence of interactions up to fourth nearest neighbours are LI_2 and DO_{22}. The two structures has identical numbers of AB nearest pairs, which means that the difference in energy is much smaller than V_1 and it is given by the anti-phase boundary energy. It has been proved rigorously by Kanamori and Kakehashi [16]from the ground state analysis of the 3d Ising model Hamiltonian that DO_{22} structure is stable if $\epsilon < 0$ and LI_2 structure is stable if $\epsilon > 0$. We find from Figure 4 that $\epsilon < 0$ at $E = E_F$ for c = 0. 75 suggesting that at this concentration DO_{22} structure is stable. A similar analysis shows that $\epsilon > 0$ for c= 0. 25 at $E = E_F$ and here the LI_2 structure is stable. This is further supported by the fact that an exchange of stability between LI_2 and DO_{22} occurs for large electron number. For c=0. 5 , the possible ground state configurations are LI_0 and A_2B_2 and we find LI_0 to be more stable by a similar analysis of anti-phase boundary energy in agreement with experiments and theoretical studies based on other methods.

Before we compare our results with other earlier works, in particular the TB-LMTO-

DCA and KKR-CPA-GPM, it is worthwhile to examine these in some detail.

The TB-LMTO-DCA shares most of the features of our TB-LMTO-ASR :

(i) Both methods employ the TB-LMTO for the description of electronic structure. Both use the first order Hamiltonian.

(ii) In both methods, calculations are carried out in real space, without resorting to any single site approximation.

(iii) Both methods use the orbital peeling method to obtain the effective renormalized pair interactions.

The main point of difference is the method of carrying out the configuration averaging involved in the definition of the pair potential. In the TB-LMTO-DCA the pair interactions ,in the grand canonical version, are obtained for several configurations randomly generated (consistent with all possible concentrations) and the averaging is done directly as a weighted sum. Because the pair interactions are integrated quantities, they are expected to converge fast with the number of configurations sampled. However, in principle, such a method cannot sample all possible realizations or, in other words, there is no surity that the thermodynamic limit has been achieved. On the contrary, in the TB-LMTO-ASR the configuration averaging is done using the Augmented Space Theorem . The subsequent termination of the recursive generation of the continued fraction of the configuration averaged Green function can be carefully controlled. The effective pair interactions obtained in our method are concentration dependent canonical interactions. A direct comparison between the effective pair interactions in the two methods is possible only for c=0.5 [18, 27].

The KKR-GPM method is distinct from these two methods. The main features of this method are :

(i) KKR is used for the description of the electronic structure. Since there is no linearization involved, the KKR method is certainly more accurate than the TB-LMTO.

PAIR INT.	TBLMTO-DCA	KKR-GPM	TBLMTO-ASR
V_1	4.2	2.0	4.3
V_2	-1.1	-0.8	-0.1
V_3	0.3	0.5	0.1
V_4	0.2	0.1	-0.2

Table 2: Effective Pair Potentials in mRyd/atom for various distances between the pairs for a 50-50 PdV alloy. TBLMTO-DCA values are taken from (9) and KKR-GPM from (26)

(ii) The single site CPA is used for the configuration averaging. The effective interactions are therefore concentration dependent.

(iii) Calculations are carried out in reciprocal space.

(iv) The effective pair interaction obtained in the GPM method are usually not renormalized, so the contributions from self-retraced paths and higher order interactions are ignored. Although in some other versions of the GPM (Tight-Binding GPM [1, 28]) the renormalization has been carried out.

In Table II we present the results for the pair interactions upto the fourth nearest neighbours obtained from different methods have been compared with our calculations for a 50-50 PdV alloy.

It is clear from the table[2] that agreement in the dominant interaction V_1 is better between the TBLMTO-DCA and our work. The reasons for this may be attributed to the fact that both TBLMTO-DCA and TBLMTO-ASR are based on the embedded cluster approach and is therefore non-perturbative. The pair-potentials obtained by these methods are renormalized compared to those obtained by the KKR-GPM. The effective interactions are very small energy differences (of the order of mRyd/atom-spin) and are

---

[2] While comparing different results one should be careful about the units used. In the KKR-GPM and our work the effective interactions are quoted in mRyd/atom-spin, whereas in TBLMTO-DCA they are quoted as meV/atom. In addition in the KKR-GPM and our work the energy expansion is in terms of concentration fluctuations, whereas in the TBLMTO-DCA the expansion is in terms of site-spin variables. This introduces a factor of 1/4 in the definition of the effective interactions.

very sensitive to the specific description of electronic structure. The KKR scheme with its non-linear secular equation is definitely more accurate than its linearized version, the LMTO.

There is greater variation in the V_2, V_3 and V_4 between the various methods.In a systematic study of PdRh alloys using different Hamiltonians : parametrized tight-binding, TBLMTO with equal Wigner-Seitz radii, TBLMTO with different Wigner-Seitz radii and one with experimental lattice constant, Wolverton *et.al.* [9] have shown that V_1 varies between -1.3 mRyd/atom and -0.34 mRyd/atom, while V_2 varies from about -.18 mRyd/atom to an almost zero positive value. This indicates that the pair interactions depend sensitively on the particular hamiltonian used and the approximation schemes used in describing the electronic structure. We expect a similar sensitivity for PdV also.

There are several underlying differences between the TBLMTO-DCA and our work.

(i) For the input to alloy calculations, the TBLMTO-DCA assumes an alloy volume which is the concentration weighted average of the volumes of pure Pd and V. The potential parameters for Pd and V are then calculated at the common Wigner-Seitz radius of the alloy. In our calculations we have taken unequal Wigner-Seitz radii for Pd and V, which takes into account charge self-consistency, as emphasized by Kudrnovský and Drchal [20].

(ii) The TBLMTO-DCA uses the precription of Shiba to obtain the off-diagonal matrix element between unlike atoms. In our work, on the augmented space, it is not necessary to use this prescription and we have built up the off-diagonal matrix element from the potential parameters Δ_i^A and Δ_j^B and the structure matrix S_{ij}^{β}.

(iii) The configuration averaging procedure is also quite different in the two procedures.

It is not surprising therefore that there is some mismatch particularly between the values of V_2, V_3 and V_4. The sign of V_4 in our work is opposite to that of TBLMTO-DCA. Recently it has been observed by Singh and Gonis [29] that changing the description of the electronic structure from KKR to KKR-ASA within the same averaging scheme,

COMPO - SITION	ORDERED STRUCTURES	KKR -GPM	TBLMTO -ASR
PdV$_3$	D0$_{22}$-L1$_2$	4.3	4.0
PdV	A$_2$B$_2$-L1$_0$	4.5	2.02
Pd$_3$V	DO$_{22}$-L1$_2$	-0.4	-0.31

Table 3: Antiphase boundary energies in mRy/atom-spin for PdV at different atomic compositions. The antiphase boundary energies for the KKR-GPM has been taken from figure 1 of (26)

there is a change in the value of V$_1$ by about 1 mRyd/atom and also a change in the sign of V$_4$.

In the TBLMTO-DCA, the charge neutrality is achieved by shifting the on-site energy of a constituent with respect to the other, such that each configurationally averaged atom is locally charge neutral. In our scheme, as explained earlier, we have used the precription of Kudrnovský and Drchal and used unequal Wigner-Seitz radii for the constituents, with charge neutrality in each of the spheres. The position of the Fermi energy depends sensitively on charge neutrality. For PdV system this is particularly important, since the number of valence electrons in the constituents are very different there could be considerable charge realignment on alloying and a small consequent shift in the Fermi level can lead to appreciable change in the pair potentials.

The quoted TBLMTO-DCA pair potentials are in the grand canonical scheme (concentration independent). In the thermodynamic limit ($N \rightarrow \infty$) the canonical and grand canonical pair potentials converge on each other. But numerical calculations [27] have demonstrated that for asymmetric systems, like PdV, the convergence is not good and this may contribute to the difference between the TBLMTO-DCA and the canonical pair potentials of our work.

In order to complete comparisons with other works, we quote the antiphase boundary energies in Table III and the ordering energies in Table IV for three different alloy compositions for PdV.

The antiphase boundary energies for the 75-25 and 25-75 alloys agree well with each

COMPO - SITION	ORDERED STRUCTURE	TBLMTO -DCA	KKR -GPM	TBLMTO -ASR
PdV_3	$L1_2$	-8.58	-6.67	-7.98
PdV	$L1_0$	-11.02	-7.40	-10.53
Pd_3V	DO_{22}	-9.8	-2.31	-8.54

Table 4: Ordering energies in mRy/atom for PdV at different atomic compositions.

other. The TBLMTO-DCA uses a grand-canonical version of the pair interactions, so that we may compare with only the 50-50 alloy case. From table 3 of [9] we may obtain a value 3.16 mRy/atom-spin which is midway between the KKR-GPM and our values.

Ordering energy [3] gives a quantitative estimate of the energy difference involved in a order-disorder transition and is the most critical test of the formalism, because it is much smaller (typically of the order of 0.1eV or smaller) than other quantities relevant to alloying, such as the formation energy of the random state which is five or more times larger. As anticipated from earlier comparisons, the agreement of our work with TBLMTO-DCA is much closer than that of the KKR-GPM. In particular, the ordering energy of the DO_{22} structure is rather small in the KKR-GPM as compared to the TBLMTO-DCA and our work. We should mention here that the TBLMTO-DCA includes higher order interactions (upto quadruplets). For asymmetric systems like PdV, inclusion of these higher order interactions may prove to be important [30]

It is interesting to note that the prediction of the stable ordered ground states for all the three concentrations is the same in all the three methods discussed.

In conclusion our results demonstrate that augmented space recursion and orbital peeling in conjunction with LMTO formalism , constitute a viable and computationally feasible approach to the calculation of phase stability in binary substitutionally disordered alloys . However , before accurate quantitative answers can be obtained , further work is necessary in order to incorporate self-consistency in the total energy , exchange and correlation effects , elastic interactions and lattice relaxation into theory of alloy

---

[3] figures for the TBLMTO-DCA have been read from Fig 2(d) of the reference [9], while those for the KKR-GPM is taken from Table 1 of [26]

phase stability. Our methodology is capable of tackling these sophistications and this will constitute the substance of our later work.

References

[1] Gonis A. ,Zhang X. G. ,Freeman A. J. ,Turchi P. , Stocks G. M. and Nicholson D. M. , Phys. Rev. **B36** 4630 (1987)

[2] Connolly J. W. D. and Williams A. R. , Phys. Rev. **B27** 5169 (1983)

[3] Ducastelle F. and Gautier F. , J. Phys. **F6** 2039 (1976)

[4] Gonis A. and Garland J. W. ,Phys. Rev. **B16** 2424 (1977)

[5] Györffy B. L. and Stocks G. M. , Phys. Rev. Lett. **50** 374 (1983)

[6] Kumar V. , Mookerjee A. and Srivastava V. K. , J. Phys. **C15** 1939 (1982)

[7] Mills R. and Ratnavararaksa R. ,Phys. Rev. **B18** 1200 (1974)

[8] Garkusha V. V. , Loś V. F. and Repetsky S. P. , Theor. and Math. Phys. **84** N1, 99 (1990) ; Loś V. F. and Repetsky S. P. , J. Phys. Condens. Matter (in press)

[9] Dreyssé H. , Berera A. , Wills L. T. and de Fontaine D. , Phys. Rev.**B39** 2442 (1989) ; Wolverton C. ,Ceder G. , de Fontaine D. and Dreyssé H. ,Phys. Rev. **B48** 726 (1993)

[10] Mookerjee A. , J. Phys. **C6** 1340 (1973)

[11] Saha T. , Dasgupta I. and Mookerjee A. , J. Phys. Condens. Matter. **6** L245 (1994)

[12] Haydock R. , Heine V. and Kelly M. J. , J. Phys. **C5** 2845 (1972)

[13] Haydock R. , *Solid State Physics* **35** (Academic Press, N. Y.) (1988)

[14] Burke N. R. , Surf. Sci. **58** 349 (1976)

[15] Andersen O. K. and Jepsen O. ,Phys. Rev. Lett. **53** 2571 (1984)

[16] Kannamori J. and Kakehashi Y. , J. Phys. (Paris) Colloq. **38** C7-274 (1977)

[17] Berera A., Phys. Rev. **B42** 4311 (1990)

[18] Asta M., Wolverton C., deFontaine D. and Dreyssé H., Phys. Rev. **B44** 4907 (1991)

[19] Heine V., *Solid State Physics* **35** (Academic Press, N. Y.) (1988)

[20] Kudrnovský J. and Drchal V. , Phys. Rev. **B41** 7515 (1990)

[21] Haydock R. , *Ph. D. Thesis* University of Cambridge (1972)

[22] Lucini M. U. and Nex C. M. M. , J. Phys. **C20** 3125 (1987)

[23] Wright H., Weightman P.,Andrews P.T., Folkerts W., Flipse C.F.J., Sawatsky G.A., Norman D. and Padmore H., Phys. Rev. **B35** 519 (1987)

[24] Bose S.K., Kudrnovký J., Jepsen O. and Andersen O.K., Phys. Rev. **B45** 8272 (1992)

[25] Saha T. , Dasgupta I. and Mookerjee A. , Phys. Rev. B (communicated) (1994)

[26] Turchi P. E. A. , Stocks G. M. , Butler W. H. , Nicholson D. M. and Gonis A. , Phys. Rev. **B37** 5982 (1988)

[27] Wolverton C., Asta M., deFontaine D. and Dreyssé H., Phys. Rev. **B44** 4914 (1991)

[28] Bieber A. and Gautier A., J. Phys. Soc. Japn. **53** 2061 (1984)

[29] Singh P.P. and Gonis A., Phys. Rev. **B** (1993)

[30] Wolverton C., Ceder G., de Fontaine D. and Dreysse H., Phys. Rev. **B45** 13105 (1992)

FIGURE CAPTIONS

Figure 1. Density of states vs Energy for Pd_cV_{1-c} alloys. (a) c=0.0 (b) c=0.25 (c) c=0.5 (d) c=0.75 (e) c=1.0. The vertical lines mark the positions of the Fermi energies.

Figure 2(a). The nearest neighbour pair potential V_1 vs band filling for Pd_cV_{1-c} alloys : full curve, c=0.5 ; dashed curve, c = 0.75; and dotted curve c=0.25. Vertical lines mark the band filling in the three different concentrations.

Figure 2(b). The nearest neighbour pair potential V_1 vs energy for Pd_cV_{1-c} alloys : full curve, c=0.5 ; dashed curve, c = 0.75; and dotted curve c=0.25. Vertical lines mark the Fermi energies.

Figure 2(c). The number of states per atom as functions of energy for the three alloys mentioned in Fig 2(a)-(b). The vertical lines mark the Fermi energies.

Figure 3. The n^{th} neighbour pair potentials vs band filling for c=0.5, full curve, n=2; dashed curve n=3 and dotted curve n=4. Vertical lines mark the band filling in the three different concentrations.

Figure 4. The antiphase boundary energies for c = (a) 0.25 (b) 0.5 and (c) 0.75 Vertical lines mark the band filling in the three different concentrations.

FIGURE.1

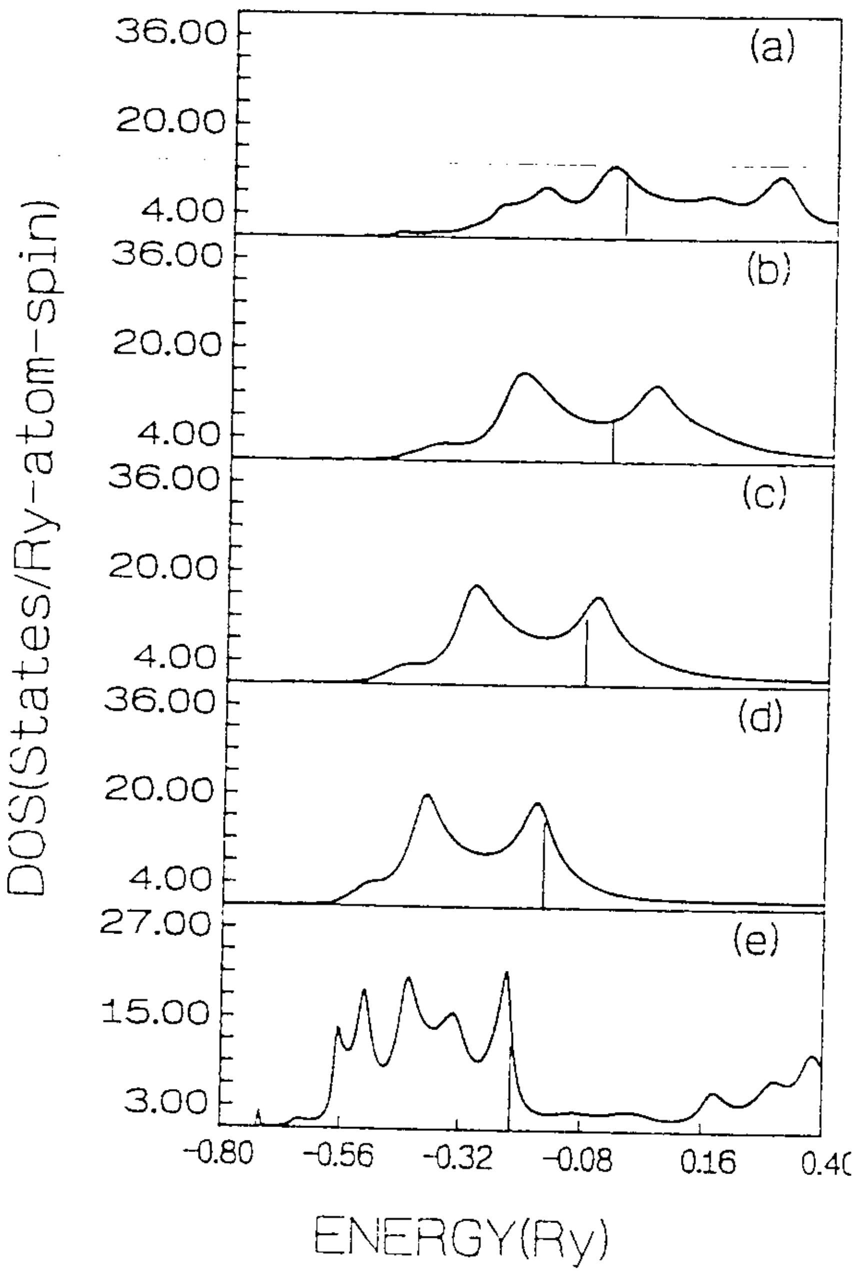
(a)
(b)
(c)
(d)
(e)
36.00
20.00
4.00
27.00
15.00
3.00
DOS(States/Ry-atom-spin)
-0.80
-0.56
-0.32
-0.08
0.16
0.40
ENERGY(Ry)

FIGURE.2(a)

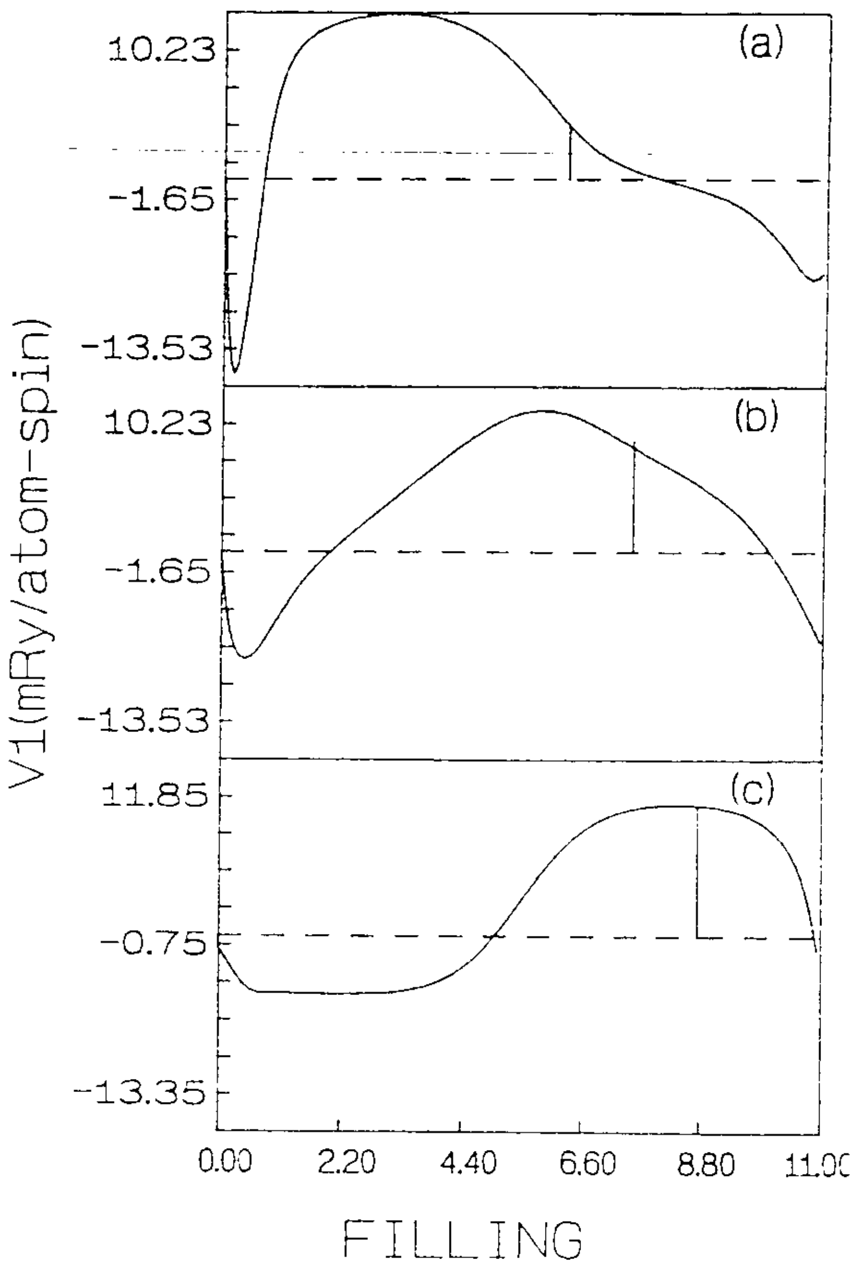

(a)
(b)
(c)
10.23
-1.65
-13.53
10.23
-1.65
-13.53
11.85
-0.75
-13.35
V1(mRy/atom-spin)
0.00
2.20
4.40
6.60
8.80
11.00
FILLING

FIGURE.3

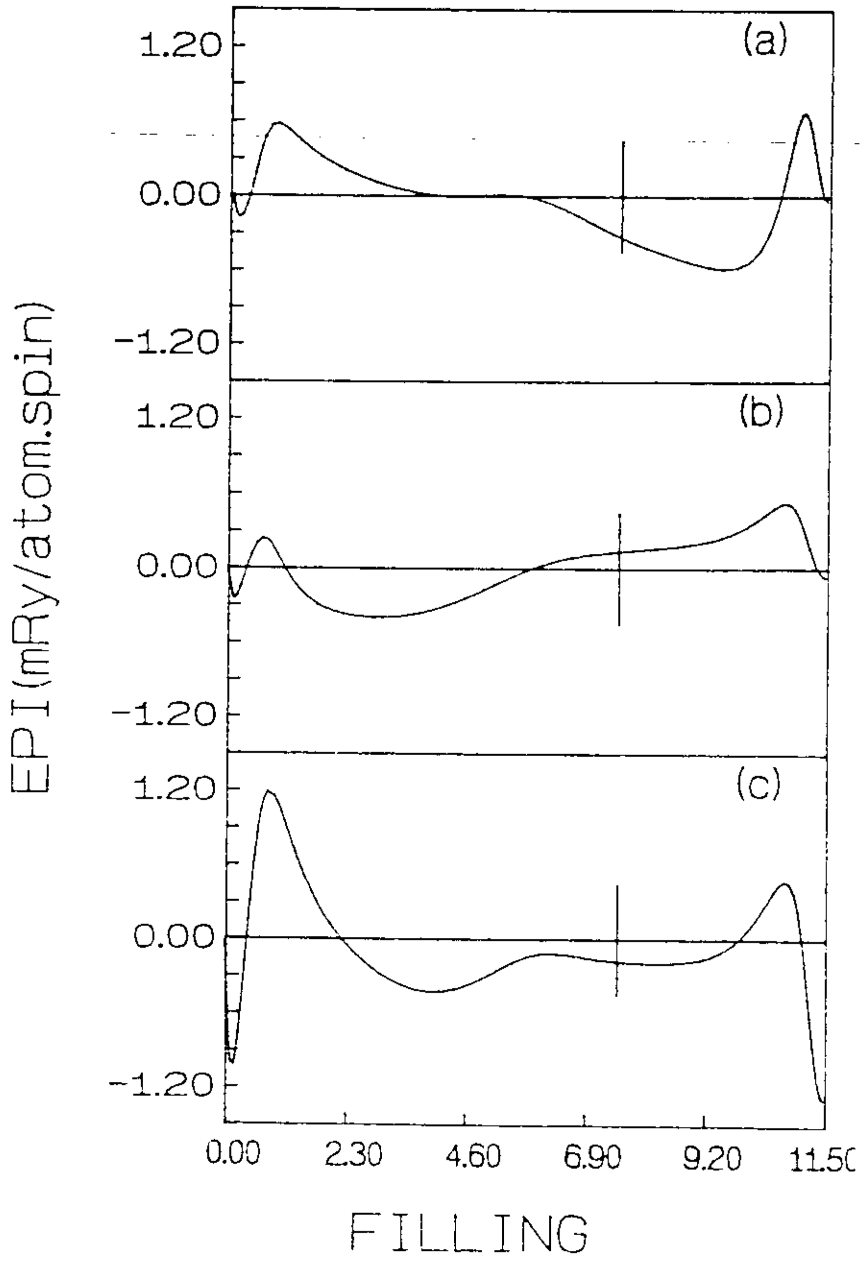
(a)
(b)
(c)
1.20
0.00
-1.20
EPI(mRy/atom.spin)
0.00
2.30
4.60
6.90
9.20
11.50
FILLING

FIGURE.4

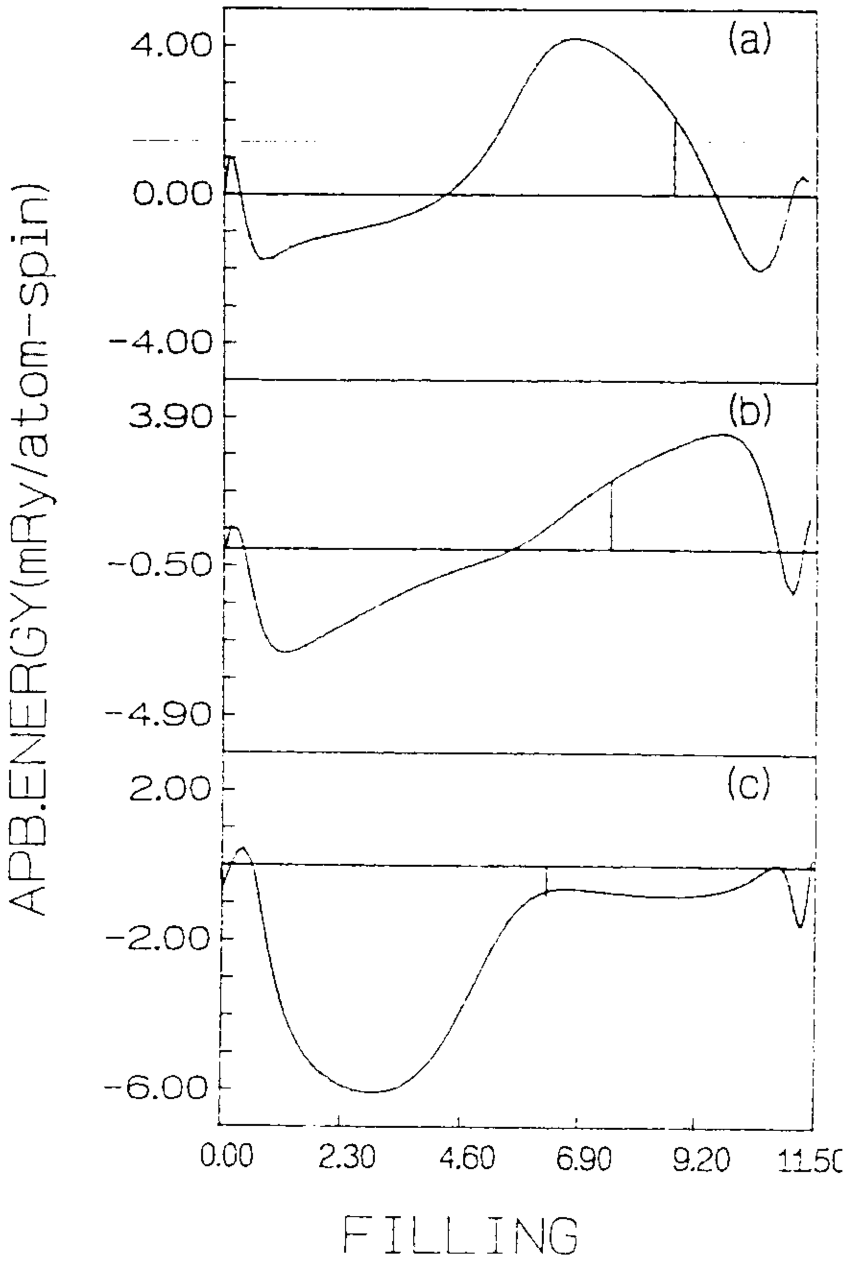
APB.ENERGY(mRy/atom-spin)
(a)
4.00
0.00
-4.00
(b)
3.90
-0.50
-4.90
(c)
2.00
-2.00
-6.00
0.00
2.30
4.60
6.90
9.20
11.50
FILLING